Temperature Dependence of thermal Conductivity of Different Geopolymer Materials for Green Building Applications

Zoltán Börcsök[1], *Roland* Szabó[2], *Gábor* Mucsi[2], *József* Faitli[2], *Thanh Tung* Nguyen[3], *Duong Hung Anh* Le[4*], *Zoltán* Pásztory[1]

[1]University of Sopron, 4 Bajcsy Zs. str., Sopron 9400 Hungary
[2]University of Miskolc, Egyetemváros, Miskolc 3515 Hungary
[3]Research Institute of Forest Industry - Vietnamese Academy of Forest Sciences, 46 Duc Thang - Bac Tu Liem - Ha Noi 100000 Vietnam
[4]Department of Mechanical Engineering, The University of Danang - University of Science and Technology, 54 Nguyen Luong Bang, Lien Chieu, Danang 550000 Vietnam

Abstract. Three types of geopolymer were produced by using flying ash, sodium hydroxide and sodium silicate for recycling the waste of coal-fired power plants. The goal was to prepare an alternative inorganic insulation material that can be used even in wet conditions and provide a substitute material for cement-based products. Thermal conductivity was investigated in different mean temperatures, ranging from −5 to 40 °C which are the most common operational temperatures in a temperate climate zone. Beside the components of the three samples, the geometrical size and distribution of voids were investigated to determine their effect to the values of thermal conductivity. Results showed that the size, the bulk density and numbers of voids greatly affected the thermal conductance. Specifically, the foam with the lowest density and smallest voids provides the best thermal insulation, with thermal conductivity values up to 18% lower across the temperature range. In contrast, foams with larger and interconnected voids showed increased thermal conductivity due to enhanced internal convection mechanisms, particularly near 4 °C. The findings highlight that controlling void size (≤ 1 mm), and preventing inter-void connectivity are critical for optimizing low-density geopolymers as insulation materials. This research contributes practical insights for designing durable, low-carbon, and moisture-resilient thermal insulation suitable for green buildings.

1 Introduction

The rational and effective use of raw materials is needed to maintain sustainable development and decrease carbon dioxide emissions. The wider usage of waste materials results the decreasing demand for primary raw materials which is a key factor for saving resources. It can be seen an abundance of waste materials available worldwide. Recycling and reusing

* Corresponding author: ldhanh@dut.udn.vn

these materials are a fundamental goal inspiring researchers to develop new technologies and materials to recycle these wastes by producing usable materials.

Coal fly ash is a byproduct of coal combustion. Power plants around the world produce 777.1 million tons annually, and disposal of it without any treatment results in contamination in landfills, water, and soil [1]. These substances are a burden on the environment but at the same time, they might be valuable raw materials for secondary utilization. There is also a need to replace conventional cement-based concrete for environmental reasons. These demands have brought geopolymers to life [2]. Each material, containing alumina and silica barrier phases like fly ash is suitable for geo-polymerization [3]. The primary application area of geopolymers is in construction but it can be used as a fire-resistant adhesive or insulation and for other purposes. Geopolymer foams (GFs) are currently in the focus of promising research in the field of porous inorganic materials because of their excellent physical, chemical, and mechanical properties, and good chemical and thermal stability [4], which allow them to be used as acoustic and thermal insulators [5], adsorbents and filters [3], membrane [6], and catalysts [7].

Fly ash has low thermal conductivity compared to concrete, but to utilize it as an insulation, its thermal conductivity must be further reduced. The thermal conductivity of fly ash-based geopolymers is around $0.3-0.6\ \mathrm{Wm^{-1}K^{-1}}$, which can be further reduced by appropriate techniques [8]. Its thermal conductivity is influenced by several factors: density, moisture content, size, and distribution of voids in the material, etc. Some researchers investigated the role of the voids and tried to manufacture geopolymers with low density, and low thermal conductivity, but with acceptable mechanical properties [6],[9]. Zhang et al. developed a material with high porosity and low thermal conductivity of $0.0511\ \mathrm{Wm^{-1}\ K^{-1}}$ using fly ash [10]. Other scholars also studied fly ash, geopolymers, and other materials and their combinations for thermal insulation [16],[10]. Thermal insulation materials could have a wider use which can distinguish more groups and parallel with this more application purposes. Classical thermal insulation materials mean low density and low thermal conductivity that are used in wall structures or unloaded structures. The other group of insulation materials should have a higher mechanical strength. Such materials can replace silica-based materials and can be applied in load bearing structures like foundations or footings.

One of the most important properties of insulation materials is their thermal conductivity. In most cases, the value of the thermal conductivity of a material is given for one pair of temperatures, although the insulation material must withstand a variety of climatic conditions (temperature, humidity) in a specific zone. There is limited information about the temperature dependence of the thermal conductivity of these materials [11], however it can be significant changes comparing the standard determined value [12].There are studies examining the effects of high temperatures on geopolymers, but this is outside the "conventional" building operating range [13].

The aim of current research is the development of new thermal insulation foam materials using waste and by-product materials as raw materials for production of stronger mechanical structures. Other objective of this research is to determine the temperature dependence of the sample and not its mechanical and any other properties. Accordingly, this study investigated the change in the thermal conductivity of three different geopolymers as a function of temperature. The temperature range studied covered most of the outdoor temperatures commonly experienced by residential buildings in the temperate climatic zone.

2 Materials and Methods

The lignite fly ash sample used for the experiments was collected from the tailings pond of the Mátra Power Station in Visonta, Hungary. The particle size distribution (PSD) of a raw

fly ash subsample was measured by a Horiba LA-950V2 laser diffraction particle size analyser in a wet mode. The main physical characteristics of raw fly ash subsample are shown in Table 1.

Table 1. Properties of raw fly ash.

Particle density (kg/m^3)	1930
x_{10} (µm)	10.3
x_{50} (µm)	48.4
x_{80} (µm)	119.6
Specific surface area (SSA, cm^2/g)	2016.2

Particle density was measured in a 0.5 litre laboratory pycnometer using isopropyl alcohol as the measuring medium. The geometric (outer) surface area (SSA) was calculated using the measured particle size distribution (PSD) data by the laser sizer software. The chemical composition and loss on ignition (LOI) of the raw fly ash subsample was determined by X-ray fluorescence spectroscopy (XRF) is given in Table 2. The main crystalline phases of raw fly ash characterized by X-ray diffraction (XRD) were quartz, albite, anhydrite, maghemite, and hematite. The amorphous phase of this sample was 52.55%.

Table 2. Chemical composition of raw fly ash.

Component	SiO_2	Al_2O_3	MgO	CaO	Na_2O	K_2O	Fe_2O_3	MnO	TiO_2	P_2O_5	SO_3	L.o.I.*
wt.%	48.10	14.42	3.34	11.76	0.37	1.66	10.97	0.17	0.49	0.26	4.50	2.88

*Loss on ignition at 950 °C

A mixture of sodium hydroxide (8M NaOH) and sodium silicate with 2.7% K_2O, 13.7% Na_2O, 25.3% SiO_2, and 58.3% H_2O was used as an alkaline solution. The ratio of NaOH:Na silicate in the activator solution was 1:3. To foam the geopolymer paste, hydrogen-peroxide (30 mass% the solution) and aluminum powder were used (Table 3). As a first step of geopolymer foam production, the fly ash and activator solution were mixed for 2 minutes in a laboratory mortar mixer. Then the foaming agent (aluminum powder or hydrogen peroxide) was added to the mixture and was mixed for 15 seconds. Then the mixture was placed in a square template 400 × 400 mm. After the moulding, the foamed mixtures were kept under laboratory conditions at 22 °C for 24 hours and subsequently, they were inserted in a drying cabinet for 6 hours at 30 °C. After the heat curing the specimens were demoulded. All lignite fly ash geopolymer foam (LFGF) specimens were made with an alkaline solution of fly ash mass ratio of 45 wt% activator and 55 wt% fly ash. The amount of foaming agents was based on the weight of fly ash in the mixture, which can be seen in Table 4.

Table 3. Composition of geopolymer foam samples

	Fly ash, (g)	NaOH, (g)	Sodium Silicate, (g)	Al powder, (g)	H_2O_2, (g)
LFGF-A	2000	409.09	1227.27	4	-
LFGF-B	2000	409.09	1227.27	-	20
LFGF-C	2000	409.09	1227.27	-	80

Table 4. Amount of foaming agent and mark of geopolymer foam specimens,

Specimen designation	Type of foaming agent	Amount of foaming agent, (wt%)
LFGF-A	aluminum powder	0.2
LFGF-B	hydrogen-peroxide	1
LFGF-C	hydrogen-peroxide	2

The porosity of the samples (Table 5) was calculated by specimen density with pores and density without pores using the following formula (1):

$$p = \left(1 - \frac{\rho_s}{\rho}\right) \times 100\% \quad (1)$$

where p is porosity (%), ρ_s is the specimen's density with pores, which was calculated by mass and volume of table (kg/m^3), ρ is the density without pores, which was determined by a pycnometer measurement (kg/m^3).

Table 5. Porosity of geopolymer foam specimens

Specimen designation	Specimen density (with pores), (kg/m^3)	Density (without pores), (kg/m^3)	Porosity, (%)
LFGF-A	435	2151	79.8
LFGF-B	1315	2202	40.3
LFGF-C	1328	2223	40.3

The distribution of voids was determined by a Tagarno high resolution light microscope on nine designated area of 30 mm by 30 mm on each geopolymer sample, which was shown in Fig. 1.

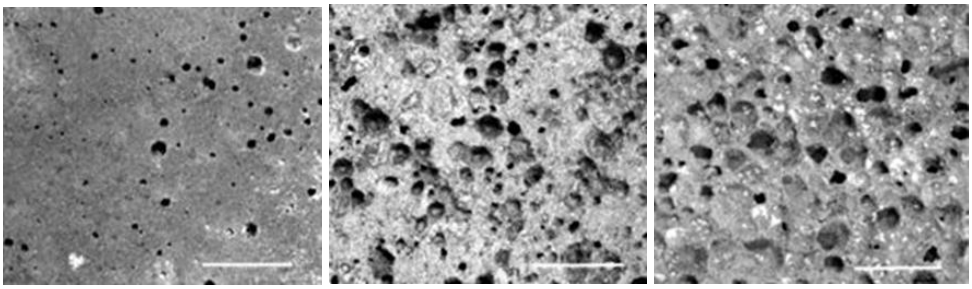

Fig. 1. Lignite fly ash geopolymer foam samples LFGF-A on the left, LFGF-B in middle and LFGF-C on the right (white lines are 1 cm length).

Before they were measured, the samples were stored at room temperature conditions (20 °C and 65% relative humidity) for 21 days. Thermal conductivity was then measured across the thickness of the panel using a custom-made heat-flow-meter apparatus (a type of hot-plate method). The thermal conductivity can be calculated at steady state conditions by measuring the heat flux, as described by Fourier's law, according to the following equation (2):

$$\lambda = \frac{d \cdot \phi_q}{\Delta T} \quad (2)$$

where λ is thermal conductivity measured in Watts per meter Kelvin ($Wm^{-1}K^{-1}$), Φ_q is measured heat flux (Wm^{-2}), ΔT is the temperature difference across the specimen (K), and d is thickness of the specimen (m).

The temperature difference between the hot and cold plate was set to 10 °C, the mean temperature ranged from −5 to 40°C and measured every 5 °C interval steps. That means the first measurement cold side temperature was −10 °C and the hot side 0 °C, in the second measurement −5 and +5 °C, and so on. For each type of panel, a thermal conductivity test was carried out on four specimens. The measurement was started when the sample reach the steady state condition which was accepted only if the fluctuation of thermal conductivity was under 0.002 $Wm^{-1}K^{-1}$. The equipment performed one measurement every minute, and the average of the last hundred measurements was accepted as the measured result of a panel. The average of the four samples data collected were taken as the result for one type of panel.

3 Results

The average thermal conductivity values of the three different panel types as a function of the mean temperature are shown in Fig. 2. For all three types have considerable change of thermal conductivity as the operational temperature change. The thermal conductivity values of the LFGF-A panel were the lowest at each measurement point, while LFGF-C recorded the highest thermal conductivity. Compared to the other two samples, the density of LFGF-A is about one third (Table 5), which explains its much lower thermal conductivity.

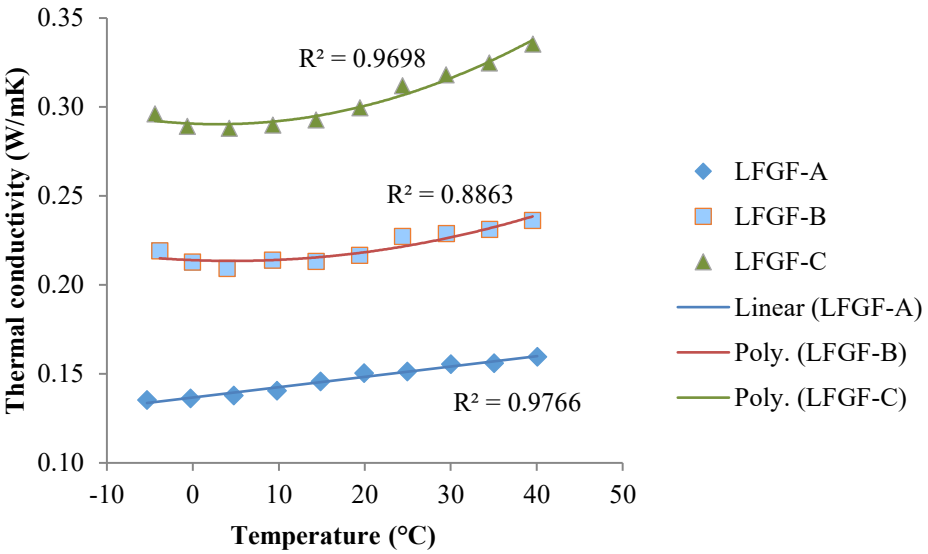

Fig. 2. Thermal conductivity values of the three-panel types as a function of the middle temperature during measurement.

The thermal conductivity results for LFGF-A are almost linear with lower conductivities at lower temperatures. There were similar trend lines results for several insulation materials [14]. The thermal conductivity difference between the lowest value compared to the highest within the measured mean temperature range was 18% for LFGF-A, 12.8% for LFGF-B, and

16.4% for LFGF-C. The LFGF-A has the smallest sized voids and shows the lowest change in thermal conductivity which suggests that the smaller bubbles mean more sophisticated material matrix which seems to be more sensitive to the change of mean temperature.

The other two types show a different behavior: both of them have the lowest conductivity at around 4 °C, below and above 4 °C their thermal conductivity increases. Berardi and Naldi found that polyisocyanurate shows a similar behavior below 10 °C [15]. They suggested that at low temperatures (lower than room temperature) by decreasing the temperature the blowing agent condensed in the voids and facilitated the heat flow. In the case of LFGF-B and LFGF-C, only hydrogen peroxide was added, so water or vapor could remain in the voids. The thermal conductivity of water/vapor increases with increasing temperature. Similarly, the thermal conductivity of ice decreases as the temperature decreases. So around 4 °C, water may condense and at lower temperatures, it was at least partially present in the form of ice, thereby affecting heat conduction.

The distribution of the voids inside the panel or the void size distribution is different in LFGF-B and LFGF-C resulting in the difference in thermal conductivity between LFGF-B and LFGF-C although these two types of panels have almost the same density and percentage of porosity. Ducman and Korat found that by increasing the amount of H_2O_2, the total number of voids decreases due to coalescence [6]. The sample LFGF-C contains a larger amount of H_2O_2 leading to a higher number of voids with connections, providing a channel for moving air (Table 6). This can explain why the thermal conductivity of sample LFGF-C is higher than that of sample LFGF-B. Sample LFGF-C has a higher number of cavities with a diameter larger than 1 mm (Figure 3) that could act as pathways for heat to flow through the material leading to an increase in its thermal conductivity by convection inside the void and the possible connection between voids.

Table 6. The number of bubbles and diameter.

	Sample	Total number of bubbles	d (mm)		
			Min	Max	Avg
LFGF-A	1	276	0.07	2.89	0.61
	2	245	0.11	2.61	0.64
	3	243	0.11	2.85	0.75
	average	**255**	**0.10**	**2.78**	**0.67**
LFGF-B	1	673	0.17	7.12	1.61
	2	590	0.25	4.92	1.46
	3	626	0.17	5.93	1.38
	average	**630**	**0.20**	**5.99**	**1.48**
LFGF-C	1	507	0.18	7.46	1.41
	2	343	0.19	7.96	1.54
	3	441	0.24	7.31	1.70
	average	**430**	**0.20**	**7.58**	**1.55**

Based on these results (Table 6), the LFGF-A sample with the lowest thermal conductivity has the lowest size of voids. Although the average size of the cavities is similar of LFGF-B and LFGF-C, however the connections between bubbles is much intense in sample LFGF-C as a consequence of higher amounts of hydrogen peroxide. These connections can be seen in Fig. 1, but cannot describe easily in distributions like in Table 6.

The average size of the cavities of LFGF-A is about half of the cavities of LFGF-B and LFGF-C. This is mainly because the distribution of LFGF-A is completely different than that of the other two types of samples. The voids sizes in LFGF-A are much smaller and the number of voids is also less.

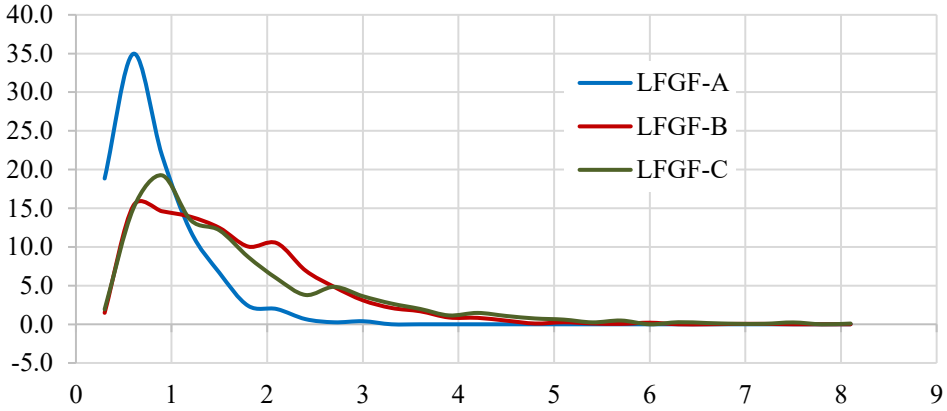

Fig. 3. Distribution of different cavity sizes in the samples.

Looking at the size distribution of the voids (Figure 3), the size of the most common voids less than 1 mm in LFGF-B and LFGF-C is similar and smaller than in the LFGF-A. While LFGF-A has very few numbers of voids over 2 mm, then the other two types of geopolymer. Figure 1 is in harmony with the Figure 3, proving the higher number of smaller voids, the smaller size of voids are much more effective from the aspect of thermal insulation, because the chance for convection is significantly less.

4 Conclusions

This study measured the thermal conductivities of three different lignite fly ash geopolymer foams: LFGF-A, LFGF-B, and LFGF-C at a range of pair temperatures. The key conclusion can be drawn from the research:

For all three types of geopolymer foams, the change in their thermal conductivities was a function of the mean temperature, and those thermal conductivity values were mostly increased with an increase in temperature.

The lowest thermal conductivity values were seen in sample LFGF-A with the lowest density and the highest number of voids under 1mm. This means low density and a smaller voids reduce the thermal conductance.

The findings that LFGF-B and LFGF-C had almost the same density and percentage of porosity, but the thermal conductivity values of LFGF-B were around 1.5 times higher than that of LFGF-C have indicated the critical role of void distribution and size within the geopolymer materials in determining their thermal conductivities. Understanding these structural aspects is vital for optimizing insulation materials and enhancing their thermal efficiency.

References

1. V.C. Pandey and N. Singh, Agric Ecosyst Environ 136, **16** (2010).
2. K.A. Komnitsas, Procedia Eng 21, **1023** (2011).
3. R.M. Novais, L.H. Buruberri, G. Ascensão, M.P. Seabra, and J.A. Labrincha, J Clean Prod 119, **99** (2016).
4. C. Bai and P. Colombo, Ceram Int 44, **16103** (2018).

5. Z. Zhang, J.L. Provis, A. Reid, and H. Wang, Cem Concr Compos 62, **97** (2015).
6. Y. Ge, X. Cui, Y. Kong, Z. Li, Y. He, and Q. Zhou, J Hazard Mater 283, **244** (2015).
7. A. Strini, G. Roviello, L. Ricciotti, C. Ferone, F. Messina, L. Schiavi, D. Corsaro, and R. Cioffi, Materials 9, **513** (2016).
8. Y. Cui and D. Wang, Advances in Materials Science and Engineering 2019, **1** (2019).
9. V. Ducman and L. Korat, Mater Charact 113, **207** (2016).
10. J. Feng, R. Zhang, L. Gong, Y. Li, W. Cao, and X. Cheng, Materials & Design (1980-2015) 65, **529** (2015).
11. M. Khoukhi, International Journal of Smart Grid and Clean Energy **217** (2019).
12. L.D.H. Anh and Z. Pásztory, Journal of Building Engineering 44, **102604** (2021).
13. L. Vickers, Z. Pan, Z. Tao, and A. Van Riessen, Materials 9, **445** (2016).
14. A.A. Abdou and I.M. Budaiwi, J. Build. Phys. 29, **171** (2005).
15. U. Berardi and M. Naldi, Energy Build. 144, **262** (2017).